Answer

Interactive comment on "High-resolution diapycnal mixing map of the Alboran Sea thermocline from seismic reflection images" by Jhon F. Mojica et al.

Anonymous Referee #2

Received and published: 11 October 2017

This manuscript presents seismic reflection data from the Alboran Sea and outlines a method for producing a map of diapycnal diffusivity across one profile. The major conclusion is that the profile shows patchy turbulence on the scale of a few kilometers horizontally and 10-15 meters vertically. Further, the authors observe greater mixing in areas of internal wave instability. Results are compared to estimates of turbulence made from XCTD and ADCP data as well as background reference models. Additional analyses of filtered slope spectra examine the relationship between diapycnal mixing and the assigned internal wave and transitional subranges.

First, we want to thank referee#2 for her/his effort. We found the comments and suggestions very useful, and we have tried to answer and/or follow all of them as indicated in our point-by-point answers below.

The introduction and background are clearly written and well presented. However, the manuscript takes on the substantial challenge of developing a new method and presenting scientific conclusions at once, and in a relatively short format. As a result, I think many issues addressing the methods, presented data, clarity of conclusions, uncertainties, and reach of results are insufficient.

Thanks for the comment. We first want to make clear that the goal of the paper is not presenting the details of the data processing and spectral analysis, nor developing a new method to estimate mixing. The method used to produce the diapycnal diffusivity map from seismic data is not new; it is analogous to that presented in previous works (i.e. Sheen et al, 2009; Holbrook et al, 2013). In addition, the seismic data and their spectra were recently processed, analyzed and interpreted in detail in another paper by our group (Sallares et al. 2016). In fact, many of the questions raised by referee#2 are addressed in this paper. We have modified the text to make it clearer in the new version of the manuscript (line 100-102, 137-141).

We would like to emphasize that our goal and original contribution of the paper are (1) producing a diapycnal mixing map of higher resolution than any previously existing one and (2) applying it for the first time to shallow waters (thermocline), a critical area to study mixing processes. We then try to interpret the observed features based on the results but also on our previous work. To do this, we use data acquired in the Alboran basin with high-resolution multichannel seismic system, which were presented, processed, analyzed and interpreted by Sallares et al. (2016). The basic points of the method applied to produce the maps are explained in this manuscript, and the details can be found in the

other two works mentioned above. We clarify this in the new version of the manuscript (lines 186-189 rewritten).

Major Concerns: Data handling and methods are insufficiently explained. The authors need to be clearer about the stated resolution. It is not accurate to apply a 1200x15 m grid to a 30x3 m grid and claim improved resolution. Many of the 30x3 m cells will not have tracks in them. In fact, at CMP spacing of 7.5 m, you can only have 4 or 5 traces represented (depending how you treat them) and few realistic and meaningful spectra can be taken at that scale.

The size of the window to calculate the spectra and to estimate the mixing values is always 1200 m wide x 15 m high. The difference with previous similar works is that the windows overlap with each other; The center of the window moves only 30 m in horizontal, and 3 m in vertical in each step. By doing this, the transition is smooth because we incorporate few new data in each new analyzed window. We can see the effect in figure rev2-1. (a) Mixing map obtained following a "conventional" way (i.e. no overlapping windows). In this case we apply a step of dx=1200 m, dz=6 m between 1200 m wide x 6 m high neighboring windows. (b) Mixing map obtained using 1200 m wide x 15 m high overlapping windows and a dx=30 m, dz=3 m step. The distribution and $k_\rho(x,z)$ values is equivalent to (a) but display smoother transitions, making the map look more "realistic". This type of representation is new, but as we stated above, the method to estimate $k_\rho(x,z)$ based on the horizontal wavenumber spectra of seismic reflectors is not new. We clarify all this in the new version of the manuscript (lines 197-199, 272-273, 298-300).

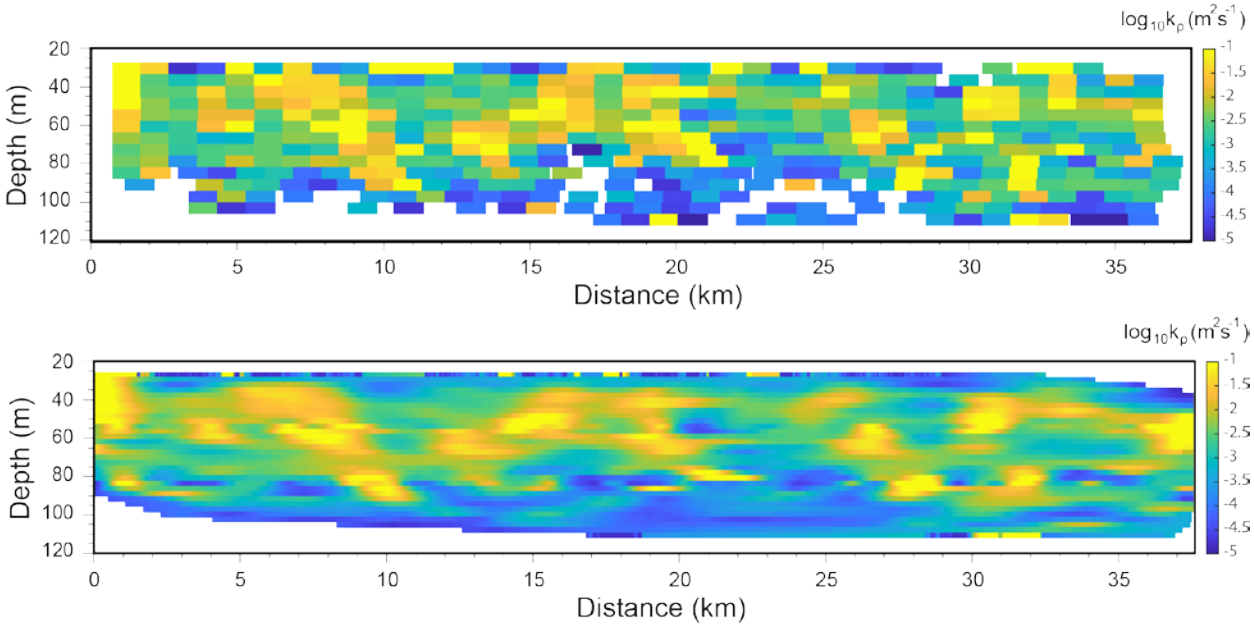

Figure rev2-1. $k_\rho(x, z)$ map obtained along the seismic profile. (a) without sliding window, using window size (1200 x 6 m) just getting one point for each window move, (b) applying sliding

window, using window size (1200 x 15m) with step (dx=30, dz=3m). The trends and values are equivalent, but (b) looks more continuous and, to us, more realistic.

The authors need to explain what happens when tracks are longer than the 1200 m box.

We cut the long tracks in 1200 m-long segments so that they fit inside the windows. This does not affect the spectrum at the spatial range analyzed. As an example, we analyze in figure rev2-2 a 16 km-long reflector (H3). We first calculate the spectrum for the whole reflector and we then split it in 10 segments (1.6 km each), and calculate their individual spectra as well as the average. The average spectra is very similar to the complete one in terms of energy and slope at the scale of interest. The details on the procedure followed to calculate the spectra can be found in Sallares et al. (2016) (line 193-194).

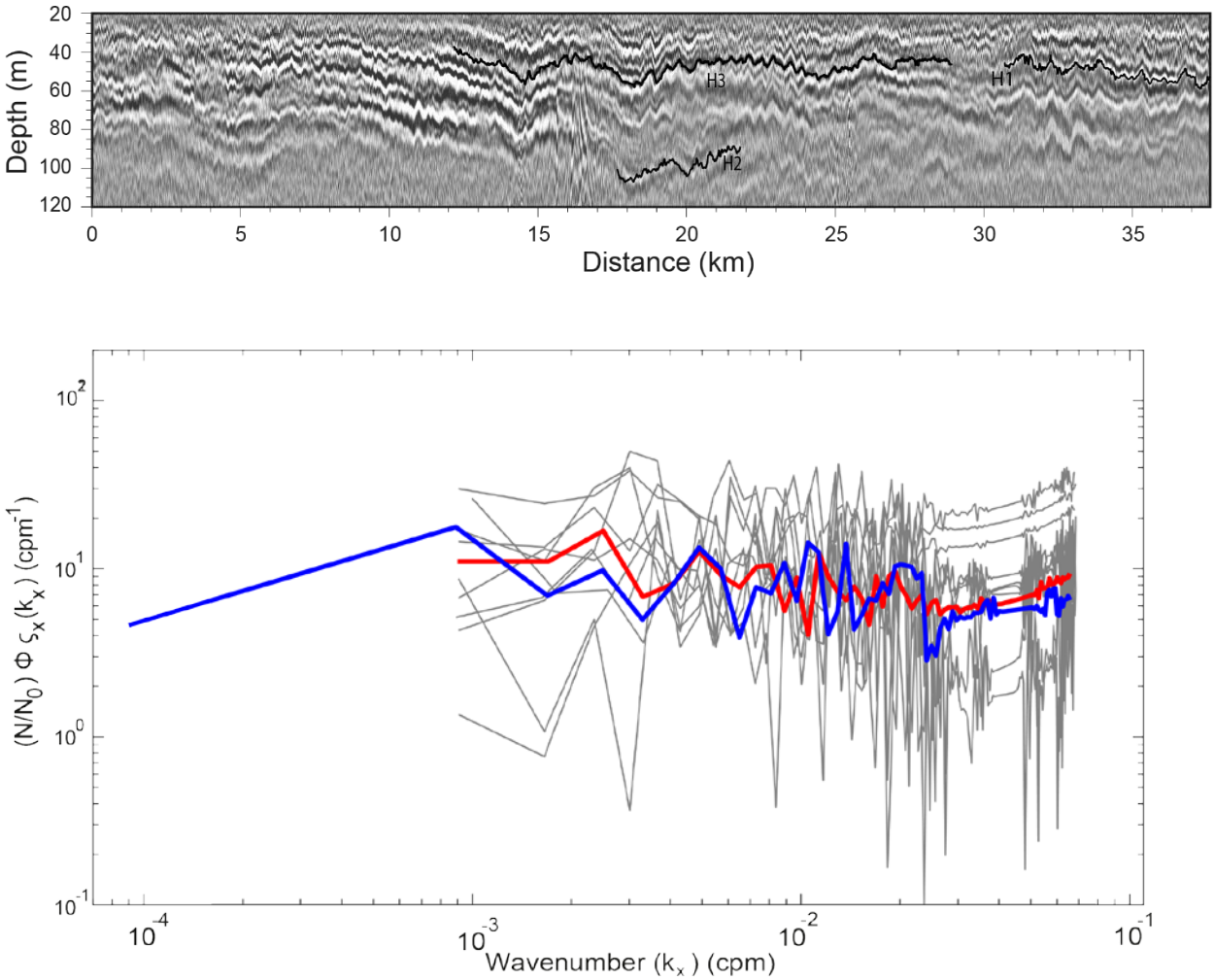

Figure rev2-2 (a) Depth-converted high-resolution multichannel seismic profile (Here we show a new horizon H3). (b) Horizontal spectrum of the vertical displacement of reflector H3. (blue line) considering the whole reflector. (gray lines) spectrum from the reflector split in ten 1.6 km-long

segments. (red line) average spectrum from the 10 segments. The average of the 10 segments and the whole reflector show the same trends in the scales of interest.

They state the tracks are 1.5-21 km long, so no tracks would fit inside the 1200 m grid length and position vertically is also unaddressed. Each track would be included in hundreds of 30x3 m grid cells which seriously undermine any claims at resolving patchy turbulence at their stated resolution.

As we already explained above: (1) 30x3m is not the grid cell, it is just the step applied to analyze a new “1200 m-long x 15 m-high” window. (2) The size of the windows (so that of the actual grid cells) is always 1200x15m. (3) The tracks longer than 1200 m are cut into smaller segments that fit inside the window.

Concerning resolution, we must distinguish between the theoretical resolution of the seismic data and that of the diapycnal mixing maps. For seismic data, the vertical resolution (i.e. the capability to discern between neighboring reflectors) is given by the Rayleigh criteria, whereas the horizontal resolution (i.e. the part of a reflector covered within half a wavelength of the seismic signal) corresponds to the first Fresnel zone. As we explain in Sallares et al. (2016), for our acquisition system, medium properties, and target depth, these are 1-2 m and 12-15 m, respectively. However, this does not represent the resolution of the mixing map. In this case, we are calculating spectra and diapycnal mixing within windows of 1200x15 m, so this could be taken as the approximate resolution of the map (in fact resolution is higher thanks to the “sliding window” approach). In summary, we do not claim that we are resolving structures of 30x3m, but the clear, larger-scale yellowish patches of 1-3 km-wide x 10-20 m-thick that are clearly identified in the map (better explained now in lines 209-212).

The authors need to show more of the data that support their methods and conclusions, particularly the reflector tracks and many more spectra.

As we explained above, our study builds on previous work concerning both method and data. The method to produce diapycnal mixing maps based on horizontal wavenumber spectra of seismic reflectors is described in Sheen et al. (2009) and Holbrook et al. (2013). The data, including acquisition system, MCS data processing, reflector tracking, S/N estimation, spectral analysis and statistical analysis of the obtained spectra, are presented in detail in Sallares et al. (2016) (in the main documents and supplementary material). We do not think that it is necessary to repeat what is already explained and shown in these papers, but we could add part of it as supplementary material if the referee and editor think otherwise (e.g. figs. Rev2-3 or 2-4). In any case, we have introduced several changes in the text to clarify this (line 100-101, 186-189).

To establish this as both a methods paper and support their science conclusion, these data must be shown and clear. First, show the 68 reflector tracks and discuss their distribution, including why application of a k value obtained on the large scale can be applied to the small scale and how to handle regions lacking tracked reflectors.

As we explained above, the original data, including the 68 reflectors and the criteria to select and track them, are shown and described in Sallares et al (2016). As you can see in figure rev2-3, they are rather homogeneously distributed throughout the analyzed area (30-110 m depth), so most of the 1200x15m analyzing windows contain reflectors and contribute to create the map. The few that do not have enough data to calculate the spectra are shown in white. We clarify this in lines 137-141.

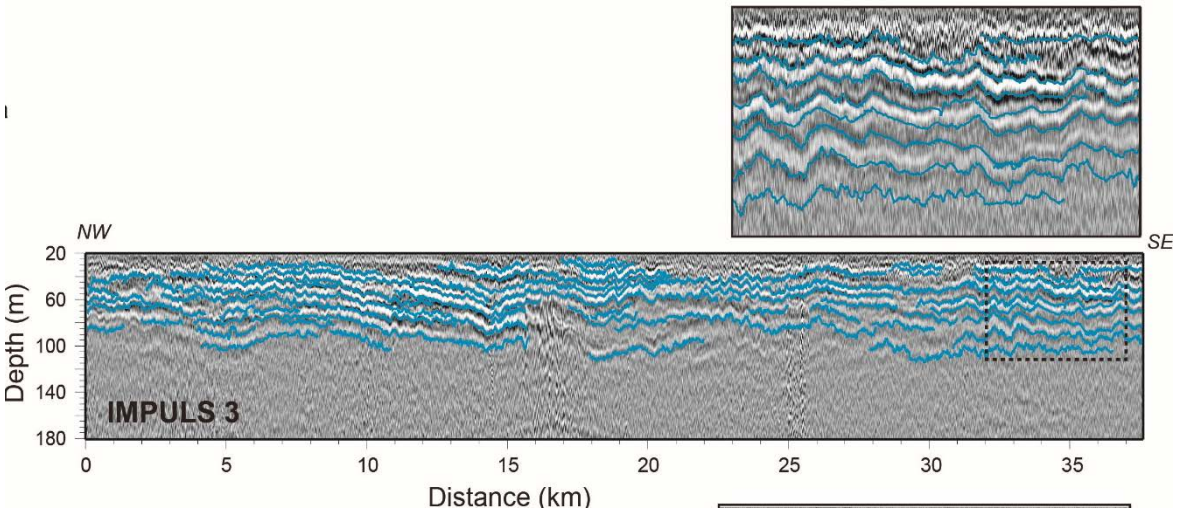

Figure rev2-3. Processed and depth-converted HR-MCS images along profile IMPULS-3, with the tracked reflectors used in the spectral analysis superimposed (blue lines). The depth range of the tracked reflectors is 30-100 m. The inset is a zoom over the area encompassed by the dashed rectangles (fig S5 in Sallares et al., 2016).

At this sub-mesoscale (~window size) we apply the Gregg89 approach (Gregg, 1989), which considers the Garret-Munk model (Garret and Munk, 1979). The observations agree with the model predictions sufficiently well to assume that it describes the link between internal waves and turbulence. The interpretation is that the model is close enough to reality to capture the principal interactions scaling the turbulent dissipation in the thermocline (line 162-165).

Second, slope spectra rely on the aggregate data of many tracks to have statistically characteristic behaviors (Klymak and Moum, 2007 part II). All of what we are shown are single-track spectra.

Several single-track spectra, as well as the combined spectra of all reflectors for two different seismic profiles including the one analyzed here, are presented in detail in Sallares et al (2016). Both the single and the combined spectra (fig rev2-4) consistently show analogous spectral slopes and slope breaks at the same horizontal scales. Additionally, the spectral slopes coincide with theoretical estimations for three different, well-known sub-regimes: the Garret-Munk model for internal waves at >100 m, Kelvin-

Helmholtz instabilities at ~100-30 m, and Batchelor model for turbulent regimes (< 30 m) (line 137-141, 150-152).

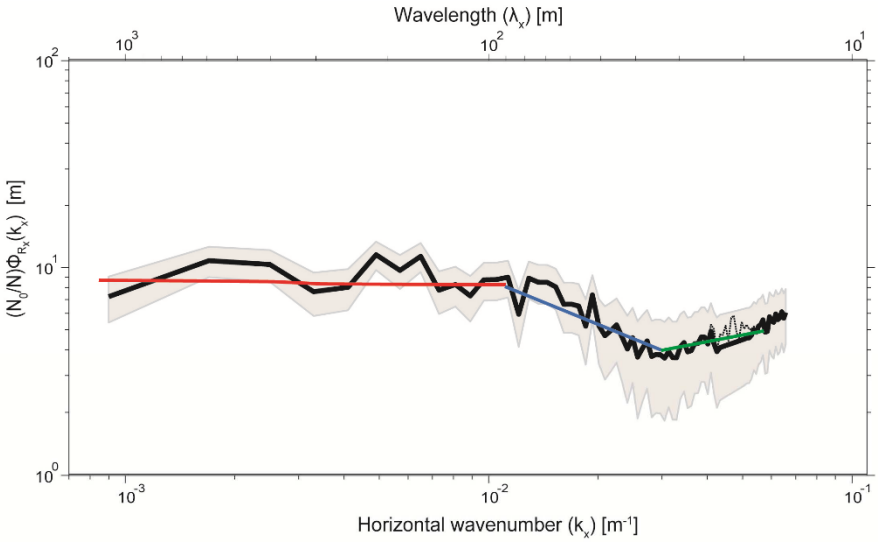

Figure rev2-4. Average horizontal spectrum of the vertical displacement, scaled by the local buoyancy, obtained for the 68 reflectors (solid line) and their corresponding 95% confidence interval (2σ) (shaded area). The reference lines are the theoretical slopes corresponding to the GM79 model for the internal wave subrange (red line), Kelvin-Helmholtz instabilities for the transitional/buoyancy subrange (blue line), and Batchelor59 model for turbulence (green line). The dashed line follows the original, unfiltered part of the spectra in the region affected by harmonic noise arising from repeated shooting. This is eliminated by applying a stop band of 0.027 to 0.021 Hz.

Third, more justification of the horizontal wavenumber bounds for the sub-regimes (IW, instability/transition, and turbulent) are needed to illustrate these are accurate bounds for sub-regimes all over the 2D line. The authors need to be clearer about the role of basic oceanographic features and the expression of turbulent structures.

This issue is also addressed in Sallares et al (2016). As it can be observed in fig rev2-4, the combined spectra of the 68 spectra show clear slope changes consistent with theoretical estimates for the three sub-regimes referred to above at precise wavenumbers (~100 m and ~30 m, respectively). The bound between the IW and shear instability regimes coincides with $l_N=2\pi\Delta V/N$, where N is the buoyancy frequency, and ΔV is the root mean square amplitude of the velocity fluctuation about the mean, which is also calculated within the targeted depth range (30-110 m) from ADCP data. The same spectral slopes and bounds are also obtained in the other seismic profile analyzed in Sallares et al (2016). This behavior also holds for most of the individual tracks. Note that otherwise we would not obtain such clear trends in the combined spectra (fig rev2-4) (137-141, 152-156).

Our interpretation in Sallares et al. (2016) is that the energy cascade between internal waves and turbulence at the sheared thermocline presents a distinct transitional subrange, possibly governed by vortex sheet dynamics. We suggest that the transition starts with the inset of shear instability along the stratified thermocline, follows with the development and rollup of KH billows, and ends with their breaking, collapse and dissipation. The energy needed to maintain these spectra comes from internal waves generated by tidal forcing at the Gibraltar strait, which are in turn subjected to a constant shear between the Atlantic and Mediterranean waters. Even though our analysis is local, the fact that the individual spectra display systematically the same transitional subrange at about the same scales, strongly suggests that this chain of processes is occurring continuously and simultaneous over the whole surveyed area (lines 150-152).

Lines 245-246 state “there is no clear visual correspondence between the k anomalies and the most obvious of the imaged oceanographic features such as IWs” which seems to be against the main thrust of the paper that sub-mesoscale features can be examined through their turbulent expressions, particularly lines 19-21 in the abstract as well as a few points in section 4.

We do not refer to all sub-mesoscale structures “in general”, but just to the internal waves that affect this region. The variations in diapycnal diffusivity show no clear correspondence with internal waves, but rather with the shear instability-like features identified in the transitional range between 100-30m (figures 7-8). We have modified the text to clarify this (line 19-21, 248-250, 339-341).

The manuscript thesis is about ocean mixing, as such, the turbulent subrange should be examined for tracks H1 and H2. Perhaps there are corresponding traits between the IW subrange and turbulent subrange, or the transitional subrange and turbulent subrange that may clarify the expression of turbulence by mesoscale and sub-mesoscale oceanographic features. Uncertainties are problematic and under addressed.

Thanks for the recommendation. We do agree and, in fact, we already examined the turbulent subrange to check if there was any correspondence between the features observed in this subrange (<30 m) and in the other two, and with the location of “mixing hotspots”. We show two examples for H1 and H2 in figures rev2-5 and 2-6, respectively. It appears that it could be (fig rev2-5d), but the problem is that this subrange is too close to the resolution limit, especially in the vertical dimension of the analyzed structures, so data are rather noisy and it does not allow extracting meaningful conclusions.

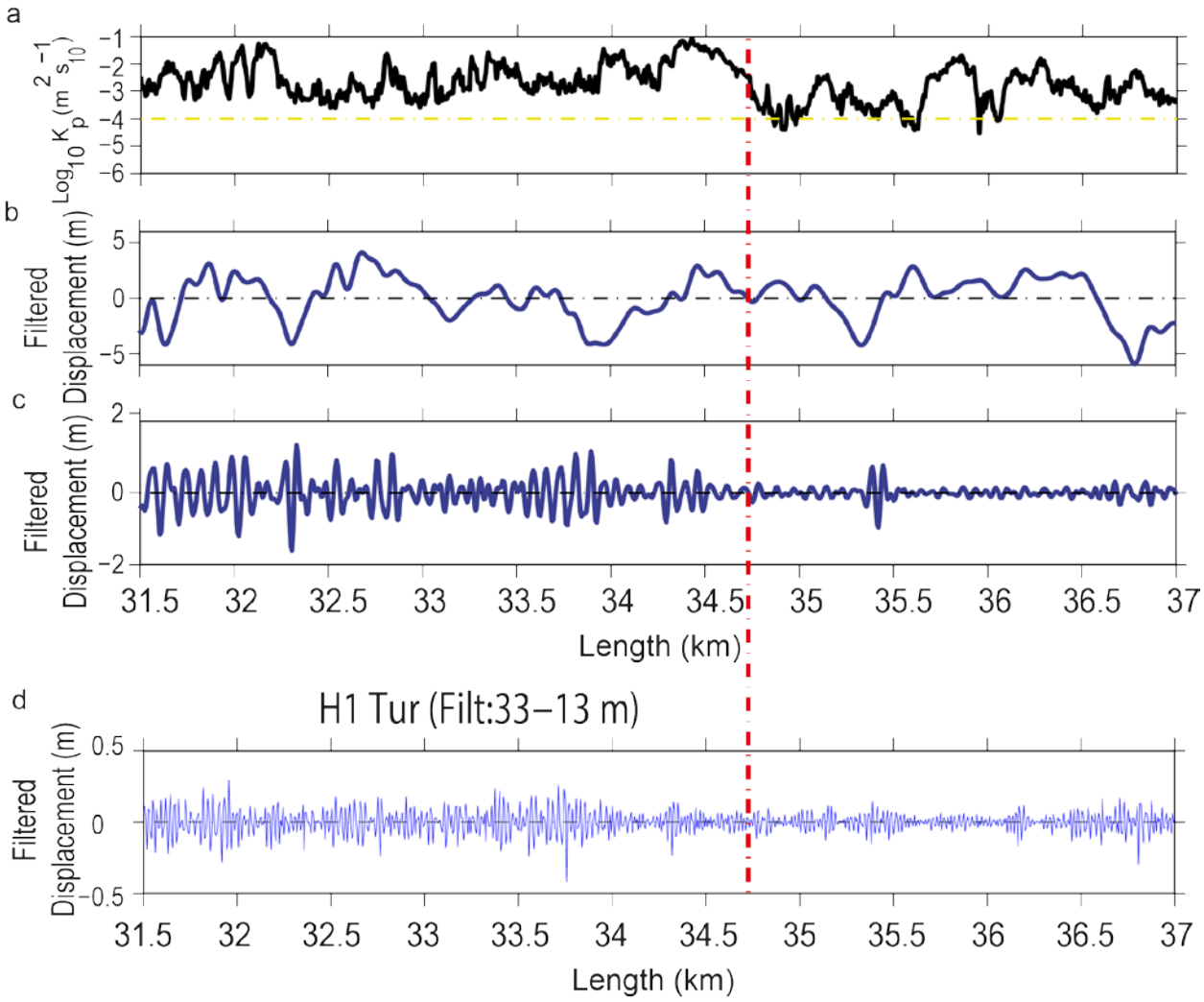

Figure rev2-5. (a) Diapycnal mixing obtained along H1 (see details of calculation in the text). (b) Signal filtered at wavelength ranges of the IW sub-range (*3000-100 m*), (c) the transitional subrange (*100-33 m*), (d) and the turbulence subrange (33-13 m). The dashed red line identifies the "breaking point" referred to in the text.

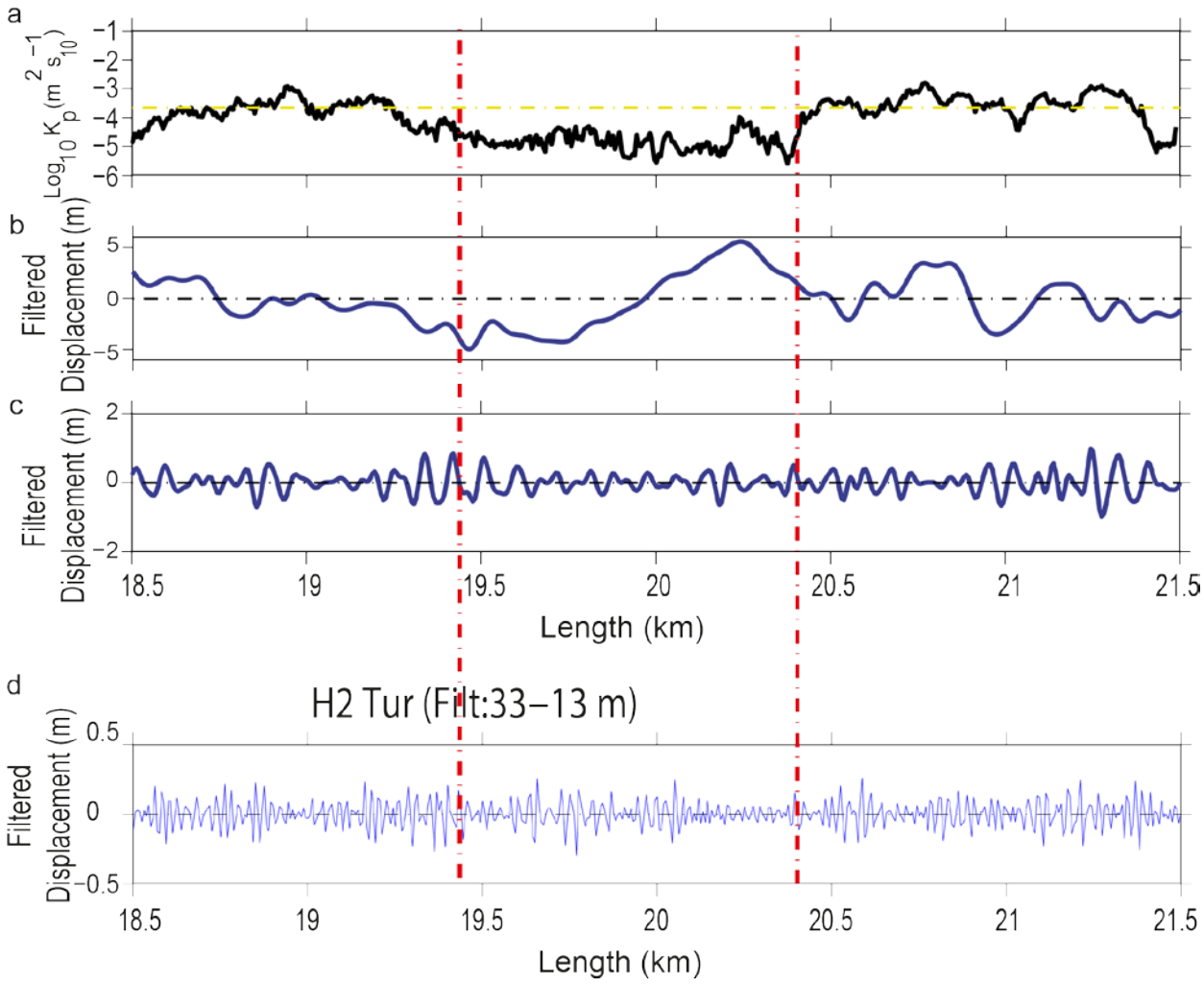

Figure rev2-6. (a) Diapycnal mixing obtained along H2 (see details of calculation in the text). (b) Signal filtered at wavelength ranges of the IW sub-range (*3000-100 m*), (c) the transitional subrange (*100-33 m*), (d) and the turbulence subrange (33-13 m). The dashed red line identifies the "breaking point" referred to in the text.

In the abstract (line 23) and conclusion (line 372) results are stated to be within uncertainty bounds but nowhere in the data do the authors show or discuss any uncertainty assessments. In section 3.2 uncertainty is briefly mentioned, but again, is simply stated that values are within uncertainty bounds. If the conclusions are supported within an uncertainty range, please show and elaborate.

Saying that the results agree "within uncertainty bounds" was an overstatement from our side. We have changed this in the new version. What we actually meant is that the global average and the values obtained with the XCTD are "within the range of values" obtained from the seismic data analysis (compare figs 4 and 5). We have reworded the text accordingly (line 22-24, 376-379).

The major conclusions for the filtered spectra analysis are under supported. Lines 378-381 deliver major conclusions about the relationship between IWs and overturning as well as shear instabilities and mixing hotspots. From the data presented, it appears these conclusions are drawn from the analysis of 2 tracked seismic reflections, H1 and H2. This overstates what is observed in the data, particularly when those two tracks were chosen as end-member individuals chosen for their position in “anomalously high (H1) and low (H2) mixing patches” (lines 264-265).

Thanks for the comment. First, we agree that the relationship between IWs and overturning is unclear and not directly justified by our results, so we have dropped this part from the text. Second, the relationship between shear instabilities and mixing hotspots comes from the analysis of various reflectors, not just H1 and H2. Here we show another reflector (H4) that show a similar pattern to H1. What we actually see is a correspondence between areas showing high diapycnal diffusivity and the location of the largest-amplitude features in the transitional domain, which we interpret to correspond to shear instabilities (possibly KH billows) based -also- on the results of Sallares et al. (2016). We have reworded lines 260-263 to clarify this.

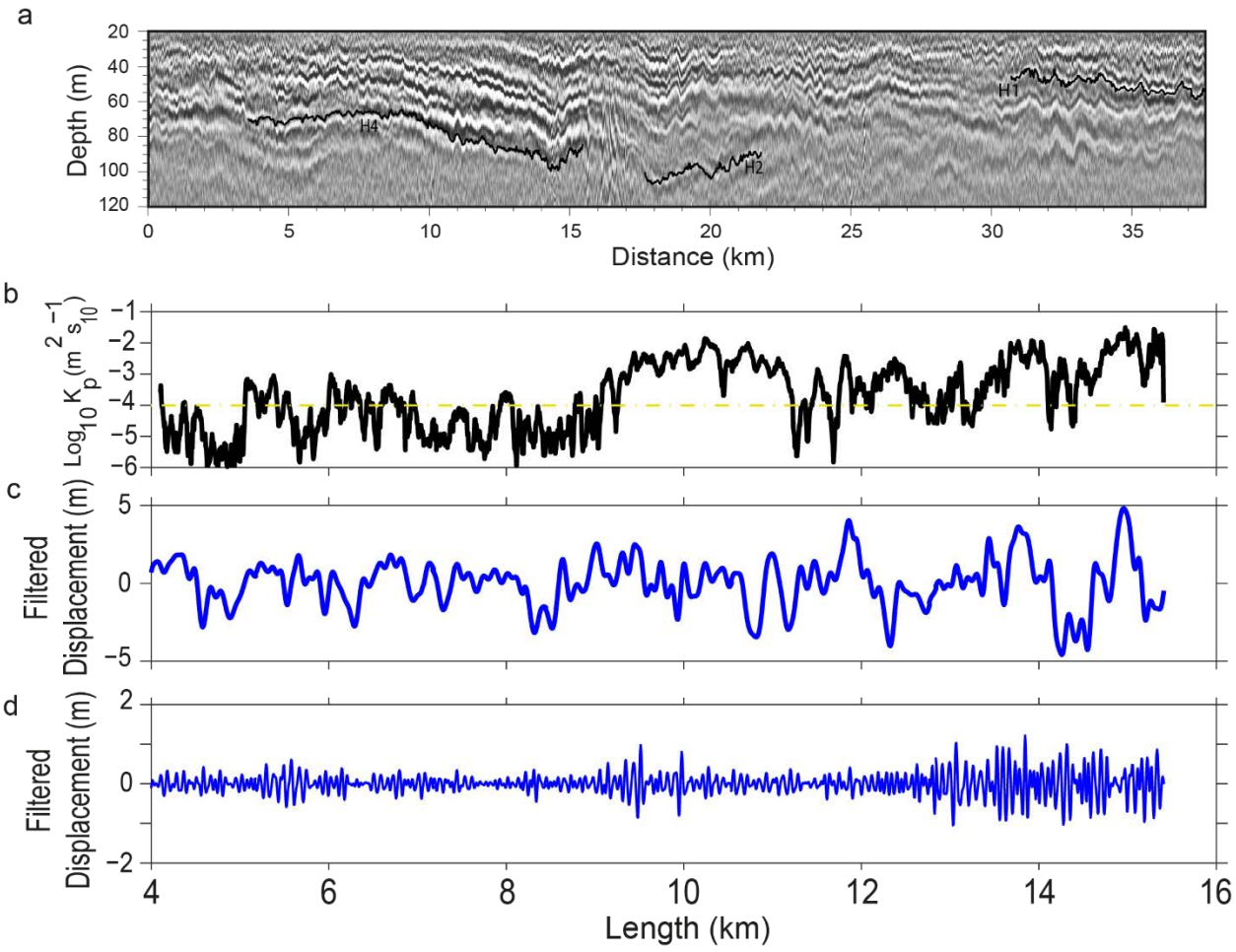

Figure rev2-7. (a) Location of H4 reflector. (b) Diapycnal mixing obtained along H4. (c) Signal filtered at wavelength ranges of the IW sub-range (*3000-100 m*), (d) the transitional subrange (*100-33 m*).

General Comments: The manuscript thesis states that authors produce a map of diapycnal mixing that show patchy nature. However, they often refer to an average k as a benchmark to compare to conventional methods. The authors need to discuss why they would average the entire map when the main thrust of the paper is that it is heterogeneous.

The average k_ρ values presented in figure 4a is just a reference to compare with the range of values that we obtain from the seismic data. This way we confirm that our values are consistent with the ones inferred using more conventional oceanographic methods (same order of magnitude). But we fully agree that the main point of our results is the patchy nature and the range of variability (of over 4 orders of magnitude) in k_ρ. In this sense, we agree that the mean MCS/XCTD values shown in fig 4 were misleading so we have deleted them and we have incorporated instead a shadowed rectangle indicating the range of values obtained in the maps, which coincide with the range of values obtained from the XCTD (new figure 4).

Additionally, the authors need to justify why just 1 XCTD and 1 ADCP data set would accurately reflect the average for their produced mixing map. For example, even if the XCTD was collected concurrently, what would the implication be if it was dropped at 8 km where k is high, or at 22.5 km where k is low?

We agree that the hydrographic data are limited. However, these are the only "quasi-synoptical" data that we have, and we think that it is valuable to incorporate them in the discussion. The fact that both the average values for the whole column as well as the range of variability obtained from the XCTD compare well with those obtained from the –completely independent- seismic data is, in our opinion, a relevant result that is worth mentioning.

Please explain how signal-to-noise is calculated. A signal-to-noise ratio of higher than 8 with 6-fold data is surprising.

As it is explained in Sallares et al. (2016), an important step towards the calculation of the slope spectra is to suppress the random noise from the data and concentrate the analysis in the frequency bands where signal is clear. This can be efficiently done by: (1) estimating the signal-to-noise ratio (S/N) in the different frequency bands, and (2) selecting and applying a band-pass frequency filter that maximizes S/N. To estimate S/N we have applied a cross-correlation-based analysis that consists of the following steps:

i) Band-pass filtering the data;

ii) Calculate the cross-correlation (CC) between each seismic trace and all its

neighbors within a distance equal to the length of the shortest reflectors used in the spectral analysis, d_{CC}=1,250 m. This is first done in the upper part of the profile (30-120 m), hence the section that we consider to contain the signal.

iii) Calculate the maximum value of the CC within a time window corresponding to the mean separation between contiguous reflectors, t_{CC} =10 ms, for each couple of traces (*MaxSigij*);

iv) Calculate the average value of *MaxSigij* for each seismic trace along the whole profile (*AvMaxSigi*);

v) Repeat steps ii) to iv) for the bottom part of the profile (120-240 m), which we consider to be noise, to obtain *AvMaxNoisei*;

vi) Calculate the ratio *S/Ni=AvMaxSigi/AvMaxNoisei* for each seismic trace;

vii) Calculate the average value of *S/Ni* for all the seismic traces: < *S/Ni*>=S/N;

viii) Repeat steps i) to vii) for the next frequency band.

Much of section 3 (first paragraph) should be expanded and put into section 2

Ok, we have done this.

Please explain why tracks H1 and H2 were analyzed with 1 km windows when the turbulent maps were analyzed with 1.2 km windows. The difference in these windows change the wavenumber range of the IW spectra and might aid some of the confusion around the handling of internal waves in the manuscript.

It was a typo. The window size for H1 and H2 is the same as in the map (1.2 km-wide) (line 272, 299).

Further, why limit the analysis to ~1 km? If they exist, larger IWs should carry even more energy and may be important.

At the spatial scale where we focus the analysis, the variation induced at longest wavelength does not affect directly the transitional subrange, as we confirm in figure rev2-2

At many points the authors state there are “no clear correlation” or similar language between filtered spectra (e.g. lines 287, 329-331). Were correlations and statistics taken for each of the 68 tracked reflectors to support, or not, a relationship between the filtered spectra? If so, this should be a major point of the paper and have supporting figures.

No, we have not formally analyzed the statistical correlation between different signals. What we mean is that there is a visual correspondence between different features, as it happens, e.g., between high values of diapycnal mixing and large-amplitude features in

the transitional domain. We have changed the word “correlation” by less confusing ones as “visual correspondence”, or similar, in the new version of the manuscript (line 292, 336, 383).

In figure 6, please show the actual fit lines for these data. This would allow for a brief discussion in the text of how you calculate spectral energy levels beyond a reference to Sallares et al. 2016.

We have modified the figure caption and text as suggested to briefly describe the procedure as follows: Figure 6 shows the average horizontal spectrum of the vertical displacement of tracked reflectors ($\Phi\varsigma_x$) scaled by the local buoyancy frequency at the reflector depth (N/N_0) to eliminate stratification effects, and multiplied by $(2\pi k_x)^2$ to enhance slope variations (blackline). The reference lines are theoretical slopes of Garrett-Munk internal wave model [Garret and Munk, 1979] (red line), Kelvin-Helmholtz instabilities [Waite, 2011] (blue line), and Batchelor's model for turbulence [Batchelor, 1959] (green line).

Specific comments:

Line 85: Citation should be Holbrook et al., 2003.

Done

Line 175: Authors need to state and explain their choice for b the scale factor

It is the scale depth of the thermocline, where we focus the analysis and where we identified the internal waves.

Lines 329-330: Suggest rewording. The authors infer IW-induced mixing is not efficient enough to keep the overturning in this dataset, I do not think the data shown makes it clear, particularly on a global scale.

Reworded to reflect better the results.

Line 340: Suggest rewording. A smooth seafloor likely suggests a lesser role in the generation of hotspot mixing, if it is disregarded entirely, please explain.

Done